Postprint of: Pladzyk A., Baranowska K., Dziubińska K., Ponikiewski Ł., One dimensional coordination polymers generated from Cd(II) tri-tert-butoxysilanethiolates and flexible aliphatic diamines, Polyhedron, Vol. 50, Iss. 1 (2013), pp. 121-130, DOI: 10.1016/j.poly.2012.10.035

One dimensional coordination polymers generated from Cd(II) tri-*tert*-butoxysilanethiolates and flexible aliphatic diamines

Agnieszka Pladzyk*, Katarzyna Baranowska, Katarzyna Dziubińska, Łukasz Ponikiewski

Department of Inorganic Chemistry, Chemical Faculty, Gdańsk University of Technology
Narutowicza Str. 11/12, 80-233 Gdańsk, Poland

* Corresponding author. *e-mail address*: agnieszka.pladzyk@pg.gda.pl (A. Pladzyk), tel.: +48 583472329; fax.: +48 583472694.

Abstract: This work concerns the coordination chemistry of cadmium(II) tri-*tert*-butoxysilanethiolates in the presence of aliphatic diamines. Reactions of binuclear $[Cd\{SSi(OtBu)_3\}_2]_2$ with respective diamines yield five new neutral one-dimensional coordination polymers, $[Cd\{SSi(OtBu)_3\}_2(\mu\text{-}C_4H_{12}N_2)(CH_3OH)]_n$ **(1)**, $[Cd\{SSi(OtBu)_3\}_2(\mu\text{-}C_5H_{14}N_2)(CH_3OH)]_n$ **(2)** $[Cd\{SSi(OtBu)_3\}_2(\mu\text{-}C_6H_{16}N_2)(CH_3OH)]_n$ **(3)**, $[Cd\{SSi(OtBu)_3\}_2(\mu\text{-}C_7H_{18}N_2)]_n$ **(4)** and $[Cd\{SSi(OtBu)_3\}_2(\mu\text{-}C_8H_{20}N_2)]_n$ **(5)**, which adopt different spatial chain topologies. New polymers are fully characterized by X-ray single-crystal diffraction, elemental analysis and IR spectroscopy. The thermal stability of **(1)**, **(3)** and **(4)** complexes is studied by thermogravimetry (TG, DTG).

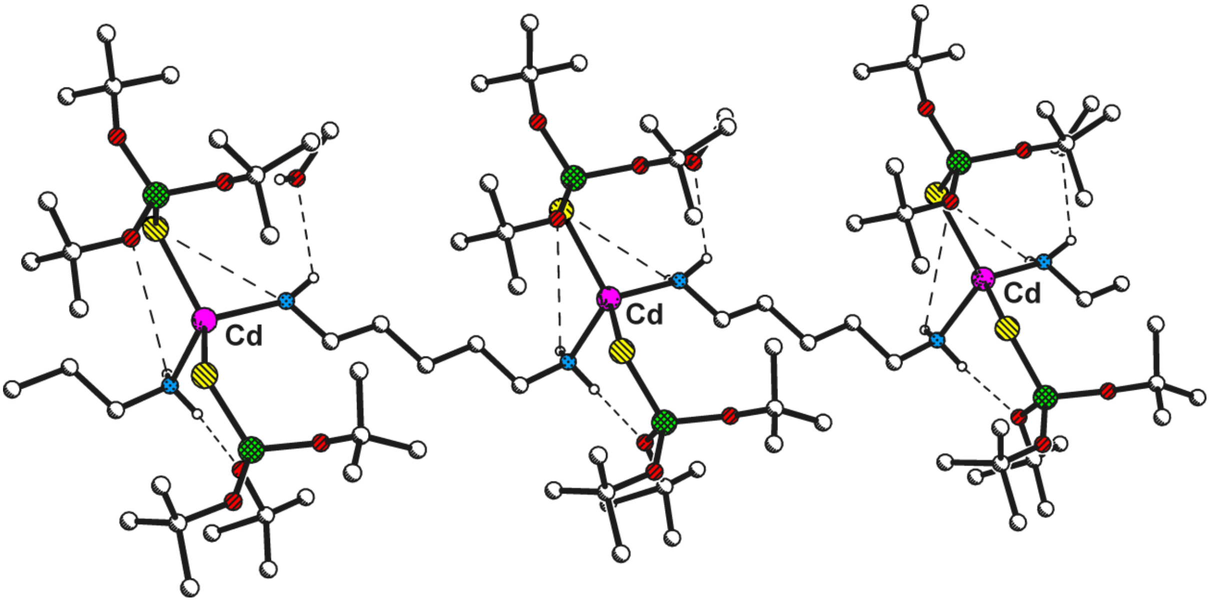

Keywords: Coordination polymers; Silanethiolates; Cadmium; Aliphatic diamines; Bridging ligands; Thermogravimetry.

1. Introduction

Complexes of d^{10} metal ions for instance cadmium arouse considerable attention of the researchers. The flexibility of stereochemistry and ability to coordinate various types of ligands lead to cadmium compounds that exhibit interesting structural features and potential applications for instance in light emitting diodes (LEDs), biomedical analyses, fluorescence, cancer phototherapy, gas adsorbents or catalysts [1-12].

The designing of artificial self-assembling systems requires the deep knowledge of many factors, such as the preference of metal ions for specific coordination environment, ligand geometry and relative orientation of donor groups as well as reaction conditions *e.g.* temperature of the synthesis or solvent polarity [13-17].

In the synthesis of various organic-inorganic networks the most extensively explored are bipyridyl derivatives which play the role of rigid linkers. Because of their abundant coordination modes to metal ions they allow to obtain diverse structural topologies with transition metals as well as complicated supramolecular networks through aromatic interactions [18-20].

For many years we have been interested in syntheses of metal complexes that contain silanethiolate residues. The most investigated silanethiol is sterically hindered tri-*tert*-butoxysilanethiol $(t\mathrm{BuO})_3\mathrm{SiSH}$ which is relatively stable in atmospheric conditions [21] and applied as a S-ligand in syntheses of complexes enables to obtain numerous mono-, bi- and polynuclear metal tri-*tert*-butoxysilanethiolates [22-31]. This particular silanethiol was used in synthesizing biomimetic complexes that imitate the structure and geometry of active sites found in some metalloproteins [32-40] as well as in the design and construction of the coordination polymers. We have carried out reactions of Co(II), Cd(II) and Zn(II) tri-*tert*-butoxysilanethiolates with bidentate 4,4’-bipy, pyrazine and quinoxaline and so far, we have obtained only one coordination polymer $[\mathrm{Co}\{\mu\text{-SSi}(^t\mathrm{BuO})_3\}\{\mathrm{SSi}(^t\mathrm{BuO})_3\}(\mu\text{-4,4'-bipy})]_n$ and several binuclear silanethiolates with metallic centers bridged by bidentate ligands [41-44]. Recently, we have considered nonrigid ligands like aliphatic diamines to be excellent candidates as building elements in the multidimensional networks. Their conformational flexibility and ability to act as H-bond acceptors and donors may lead to the formation of supramolecular structures with unusual topology structures. For our experiments we choose bimetallic and neutral cadmium tri-*tert*-butoxysilanethiolate $[\mathrm{Cd}\{\mathrm{SSi}(\mathrm{O}t\mathrm{Bu})_3\}_2]_2$ [45] and the group of flexible aliphatic diamines varying with the number of carbon atoms in chain in purpose of checking whether there are some structural relationships between the length of the flexible chain of N-donor ligands used in syntheses and topologies of potentially obtained complexes.

Despite the wealth of experimental data of bipyridyl complexes there is nothing about the use of aliphatic diamines for construction of the coordination polymers. Moreover, there is no information about compounds that contain thiolate residues and aliphatic diamines coordinated simultaneously to a metallic centre. There is only *Saber’s* work describing three 1D cadmium thiocyanato complexes with SCN residue as bridging elements [46].

As a result of our experiments we have obtained five novel and neutral heteroleptic cadmium tri-*tert*-butoxysilanethiolates with polymeric structures and bidentate aliphatic diamines as linkers. Herein we describe their syntheses, crystal structures, spectral and thermal analysis. All obtained complexes are stable in atmospheric conditions and show various spatial arrangements of polymeric chains.

2. Experimental

2.1. Materials

Tri-*tert*-butoxysilanethiol and $[Cd\{SSi(OtBu)_3\}_2]_2$ were synthesized as reported previously [21, 45]. All other starting materials were obtained from commercial sources without further purification.

2.2. Synthesis

Complexes **(1)-(5)** were obtained using the same synthetic procedure. To a solution of $[Cd\{SSi(OtBu)_3\}_2]_2$ (1.34 g, 1 mmol) dissolved in 20 mL of methanol respective amine [**(1)** 1,4-diaminabutane (0.21 mL, 2 mmol), **(2)** 1.5-diaminapentane (0.24 mL, 2 mmol), **(3)** 1,6-diaminahexane (0.24 g, 2 mmol), **(4)** 1,7-diaminaheptane (0.24 g, 2 mmol) and **(5)** 1,8-diaminaoctane (0.29 g, 2 mmol)] was added. Resultant mixtures were left at room temperature for a few days to yield colorless crystals of **(1)-(5)** complexes, stable in atmospheric conditions.

2.2.1. $[Cd\{SSi(OtBu)_3\}_2(\mu\text{-}C_4H_{12}N_2)\cdot(CH_3OH)]_n$ **(1)**

Anal. Calc. for $C_{29}H_{68}S_2Si_2O_7N_2Cd$: C 44.00; H, 8.91; S, 8.10; N, 3.54%. Found: C 44.02; H, 8.70; S, 8.40; N, 3.68%. M. p. 163-164°C. IR (solid state): ν = 3321 (s), 3261 (s), 3170 (s), 2982 (vs), 2928 (vs), 2871 (s), 1591 (s), 1471 (s), 1386 (vs), 1362 (vs), 1239 (vs), 1177 (vs), 1042 (vs, br), 1014 (vs), 965 (vs), 911 (m), 822 (s), 802 (s).

2.2.2. $[Cd\{SSi(OtBu)_3\}_2(\mu\text{-}C_5H_{14}N_2)(CH_3OH)]_n$ **(2)**

Anal. Calc. for $C_{30}H_{72}S_2Si_2O_7N_2Cd$: C 44.73; H, 9.00; S, 7.96; N, 3.48%. Found: C 44.69; H, 8.98; S, 7.98; N, 3.47%. M. p. 175-176°C. IR (solid state): ν = 3329 (s), 3261 (s), 3179 (w), 2975 (vs), 2935 (vs), 2898 (s), 1600 (s), 1471 (s), 1388 (vs), 1362 (vs), 1240 (vs), 1193 (vs), 1057 (vs), 1137(vs), 997 (vs), 928 (w), 822 (s), 813 (m), 700(s).

2.2.3. $[Cd_2\{SSi(OtBu)_3\}_4(\mu\text{-}C_6H_{16}N_2)]_n$ **(3)**

Anal. Calc. for $C_{54}H_{124}S_4Si_4O_{12}N_2Cd_2$: C 44.45; H, 8.57; S, 8.79; N, 1.92%. Found: C 45.74; H, 8.98; S, 8.15; N, 3.51%. M. p. 153-155°C. IR (solid state): ν = 3497 (m), 3342 (s), 3267 (s), 3156 (w), 2969 (vs), 2928 (vs), 2863 (vs), 2704 (w), 1630 (s), 1590 (s), 1470 (s), 1387 (vs), 1363 (vs), 1238 (vs), 1186 (vs, br), 1017 (vs, br), 1014 (vs), 908 (m), 819 (s), 801 (s).

2.2.4. $[Cd\{SSi(OtBu)_3\}_2(\mu\text{-}C_7H_{18}N_2)]_n$ **(4)**

Anal. Calc. for $C_{31}H_{72}S_2Si_2O_6N_2Cd$: C 46.45; H, 9.05; S, 8.00; N, 3.49%. Found: C 46.39; H, 8.98; S, 8.01; N, 3.50%. M. p. 152-154°C. IR (solid state): ν = 3337 (s), 3302 (s), 3260 (s), 3237 (m), 3133 (w), 2972 (vs), 2927 (vs), 2870 (s), 2764 (w), 2699 (w), 1586 (s), 1471 (s), 1456 (s), 1386 (vs), 1361 (vs), 1239 (vs), 1187 (vs), 1056 (vs), 1042 (vs), 1022 (s), 1001 (vs), 987 (vs), 909 (m), 820 (s), 802 (s), 747 (w), 725 (w).

2.2.5. $[Cd_2\{SSi(OtBu)_3\}_4(\mu\text{-}C_8H_{20}N_2)]_n$ **(5)**

Anal. Calc. for $C_{56}H_{128}N_2O_{12}S_4Si_4Cd_2$: C 45.23; H, 8.67; S, 8.62; N, 1.88%. Found: C 45.35; H, 8.68; S, 8.61; N, 1.91%. M. p. 139-140°C. IR (solid state): ν = 3342 (m), 3278(m), 2977 (vs), 2933 (vs), 2887 (s), 1727(w), 1589 (s), 1474 (s), 1388 (vs), 1364 (vs), 1241 (vs), 1186 (vs), 1103 (w), 1043 (vs), 1019 (s), 933(m), 825 (s), 824 (s).

2.3. Thermal analysis coupled with IR

Thermogravimetric analysis was performed using Netzsch thermobalance TG 209 coupled with Bruker IFS66 FTIR spectrometer under argon. The volatiles evolving from the heated sample were transported to the spectrometer chamber via thermostated pipe in the stream of argon.

2.4. Spectral measurements

The elemental analyses (C, H, S and N contents) were performed on an Elemental Analyser EA 1108 (Carlo Erba Instruments). The IR spectra were measured for crystalline compounds in the range of 4000-700 cm^{-1} with Momentμm microscope (IR detector) attached to Mattson Genesis II Gold spectrometer (IR source).

2.5. Structure determination

Experimental diffraction data were collected on a KM4CCD kappa-geometry diffractometer, equipped with a Sapphire2 CCD detector. An enhanced X-ray MoKa radiation source with a graphite monochromator was used. Determination of the unit cells and data collection were carried out at 120 K. Data reduction, absorption correction and space group determination were made using CrysAlis software package [47].

All H atoms connected to carbon atoms were placed in calculated positions guided by difference map. The C–H bond distances were constrained to the range from 0.96 to 1.00 Å, and U_{iso} = 1.2 Ueq (1.5 for methyl group), thereafter refined as riding.

In complex **(1)** one molecule of 1,4-diaminobutane was found to be disordered over two positions with occupancy factors of 0.5. Certain C atoms of 1,4-diaminobutane molecule were made equal during the refinement [EADP C27 C28 C29 C30]. This molecule was refined with the DFIX restraint due to stabilize the whole molecule of 1,4-diaminobutane (1.400 Å for N–C and 1.450 Å for C–C). The second molecule of 1,4-diaminobutane was also found over two positions with occupancy factors of 0.21(4) and 0.79(4). Atoms EADP C25 C25a and EADP C26 C26a were made equal during the refinement. The methanol molecule was found to bed disordered over two positions with occupancy factors 0.5. Two pairs of atoms O8-O8A and C31-C31a were made equal during the refinement (EADP). The methanol H atoms were located from a difference map, fixed at 0.84 Å for O–H and refined with the DFIX restraint. The amine H atoms were located from a difference map and for N1, N1A, N3 fixed at 0.88 Å for N–H and refined with the DFIX restraint. Structures of **(2)**-**(5)** complexes were solved by direct methods and all non-hydrogen atoms were refined with anisotropic thermal parameters by a full-matrix least squares procedure based on F^2. Hydrogen atoms were usually refined using an isotropic model with U_{iso}(H) values fixed to be 1.5 times U_{eq} of C atoms for CH_3 or 1.2 times U_{eq} for CH_2 groups. Only hydrogens of NH bonds in **(2)**-**(4)** were positioned from differential electron-density maps and refined freely. Disordered *t*Bu groups: C12 (*s.o.f.* 0.52(10)/0.48(10)); C15-C16 (*s.o.f.* 0.59(2)/0.41(2)); C18-C20 (*s.o.f.* 0.507(9)/0.493(9)) in (**2**), C42-C44 (*s.o.f.* 0.831(10)/0.169(10)) in (**3**). The C–C bond lengths in molecules of diamine in (**3**) were disordered C49-C51 (*s.o.f.* 0.527(8)/0.473(8)); C53-C54 (*s.o.f.* 0.570(13)/0.430(13)).

Solutions and refinements were carried out using the SHELX-97 [48]. Crystal data, description of the diffraction experiment, and details of the structure refinement are given in Table 1. Crystallographic data (without structure factors) for the structures reported in this paper have been deposited with the Cambridge Crystallographic Data Centre with reference numbers CCDC 826670 and 874406-874409 and can be obtained free of charge *via* www.ccdc.cam.ac.uk/data_request/cif.

3. Results and discussion

3.1. Synthesis and structural description of complexes (1)-(5)

All compounds were obtained by *in situ* reaction of cadmium(II) tri-*tert*-butoxysilanethiolate $[Cd\{SSi(OtBu)_3\}_2]_2$ [45] with the corresponding N-donor aliphatic diamine in solution of methanol. Syntheses resulted with air-stable and colorless crystal products insoluble in common organic solvents and water, due to their polymeric and neutral nature.

X-ray analysis performed on a single crystal of $[Cd\{SSi(OtBu)_3\}_2(\mu\text{-}C_4H_{12}N_2)\cdot(CH_3OH)]_n$ **(1)** (Fig. 1) revealed that it crystallizes in monoclinic space group $P2_1/c$ with four molecules in the unit cell.

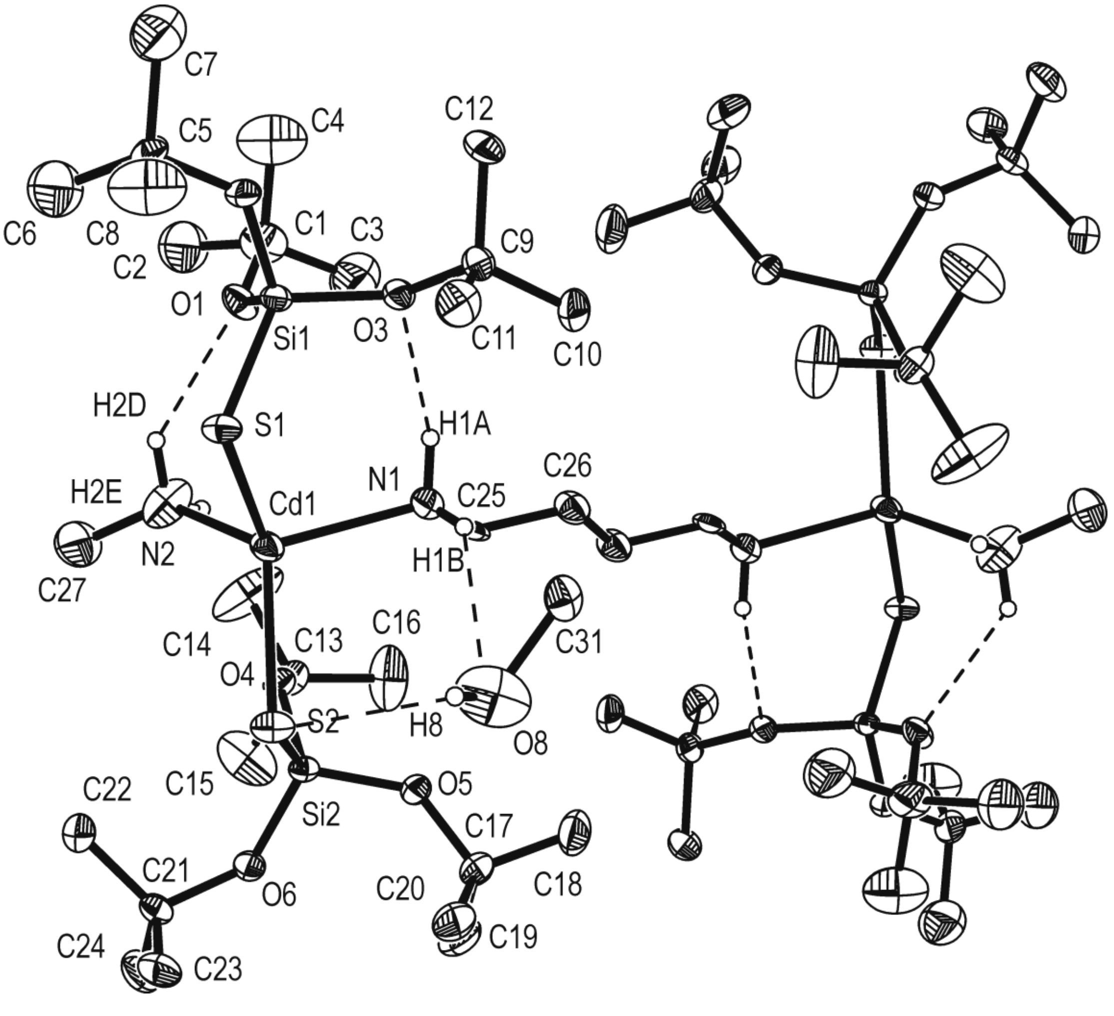

Fig. 1. Molecular structure of $[Cd\{SSi(OtBu)_3\}_2(\mu\text{-}C_4H_{12}N_2)\cdot(CH_3OH)]_n$ **(1)** with atom labeling scheme and hydrogen bond interactions (shown as dashed lines) (hydrogen atoms omitted for clarity). Thermal ellipsoids are drawn at 30% probability.

The asymmetric unit contains one cadmium(II) ion, two diamine molecules, two tri-*tert*-butoxysilanethiolate residues and one molecule of solvent-methanol. Each Cd(II) center is four-coordinated by two N atoms from bridging diamines and two S atoms from terminal coordinated $(tBuO)_3SiS^-$ ligands and can be described as a distorted $\{CdN_2S_2\}$ tetrahedral geometry with the S–Cd–S angle as the widest angle among them (124.91(5)°) (Table 2). One from two hydrogen atoms of each donor group of amine molecule is engaged in the formation of intramolecular N1–H1A···O3 and N2–H2D···O1 hydrogen bonds with oxygen atoms of adjacent tert-butoxyl groups (Table 4). The molecule of methanol solvent is sited in the void between polymer chains. The resolution of the structure of **(1)** without specifying any parameters showed that the molecule of solvent is sited in two position and forms two weak N1–H1B···O8 and O8–H8···S2 hydrogen bonds (*D*···*A* 3.499 and 3.409 Ǻ respectively), however they are strong enough to keep the molecule of solvent in the structure. The resolution showed also that the molecules of linked diamines are positioned alternately in regular and disordered form, what automatically influences the distance values between consecutive cadmium atoms (10.356 Ǻ and 8.403 Ǻ respectively). The chains of **(1)** form channels running along the [010] crystallographic axis where molecules of methanol reside (Fig. 2).

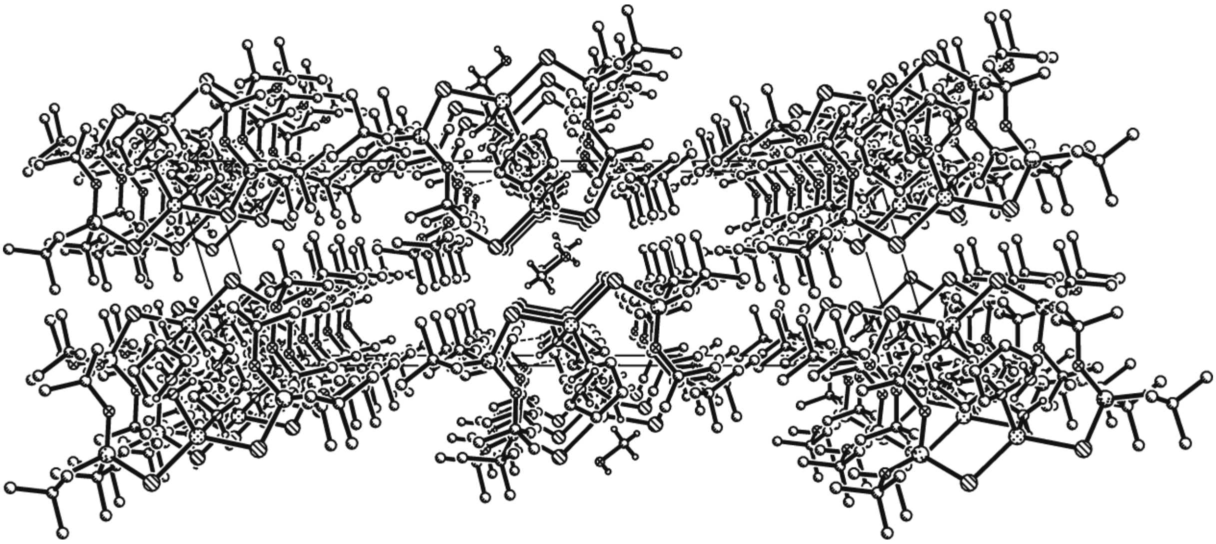

Fig. 2. Crystal packing of **(1)** along *b* axis. H atoms of *t*BuO groups omitted for clarity.

Coordination polymers of $[Cd\{SSi(OtBu)_3\}_2(\mu\text{-}C_5H_{14}N_2)(CH_3OH)]_n$ **(2)** and $[Cd\{SSi(OtBu)_3\}_2(\mu\text{-}C_7H_{18}N_2)]_n$ **(4)** crystallize in the same space group (*P*–1) with similar unit cell dimensions. The topology of their polymeric structures is common and the view of **(2)** and **(4)** is given in Figures 3 and 5. The coordination motifs around Cd atom are CdN_2S_2

just as in **(1)**, but there is also a difference between the structure of polymers **(2)** and **(4)** and it is the regular arrangement of carbon chain of 1,5-diaminepentane and the presence of solvent molecule in **(2)** (Fig. 3) and all Cd atoms laid in one line distant by 10.039 Ǻ.

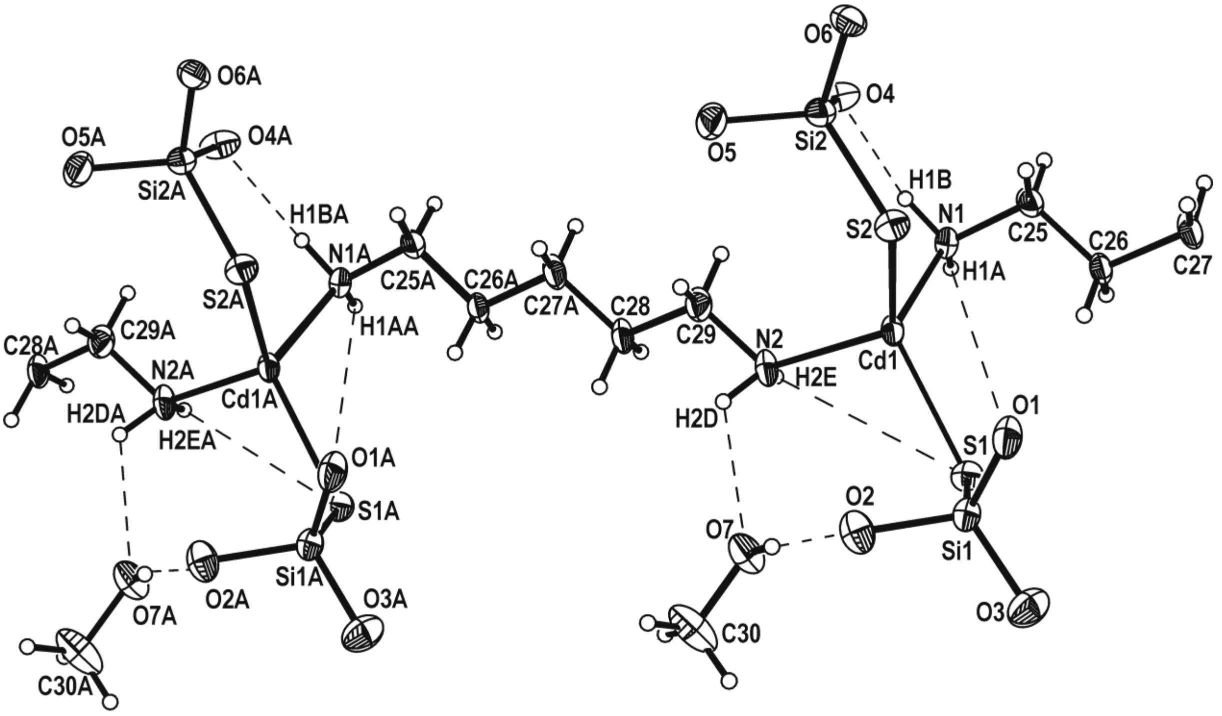

Fig. 3. Molecular structure of $[Cd\{SSi(OtBu)_3\}_2(\mu\text{-}C_5H_{14}N_2)\cdot(CH_3OH)]_n$ **(2)** with atom labeling scheme and hydrogen bond interactions (shown as dashed lines). All *t*Bu groups are removed for clarity. Thermal ellipsoids are drawn at 30% probability.

A close look at the structure of **(2)** showed the presence of intra- and intermolecular hydrogen bonds: two intramolecular N1–H···O are formed by hydrogen atoms H1A and H1B of diamine with O(1) and O(4) of two *t*BuO groups. One of two hydrogens of the second nitrogen N2 is engaged in one intramolecular N2–H2E···S1 hydrogen bond with sulfur atom of the silanethiolate residue, whereas the second one forms one intermolecular N2–H2D···O7 hydrogen bond with methanol molecule (Table 4). Hence, neighboring threads of polymer **(2)** are arranged parallel and adopt the shape of ribbons (Fig. S2 Supplementary Materials). The molecule of solvent is trapped in the structure by the formation of additional O7–H7D···O3 hydrogen bond with oxygen atom of *t*BuO group.

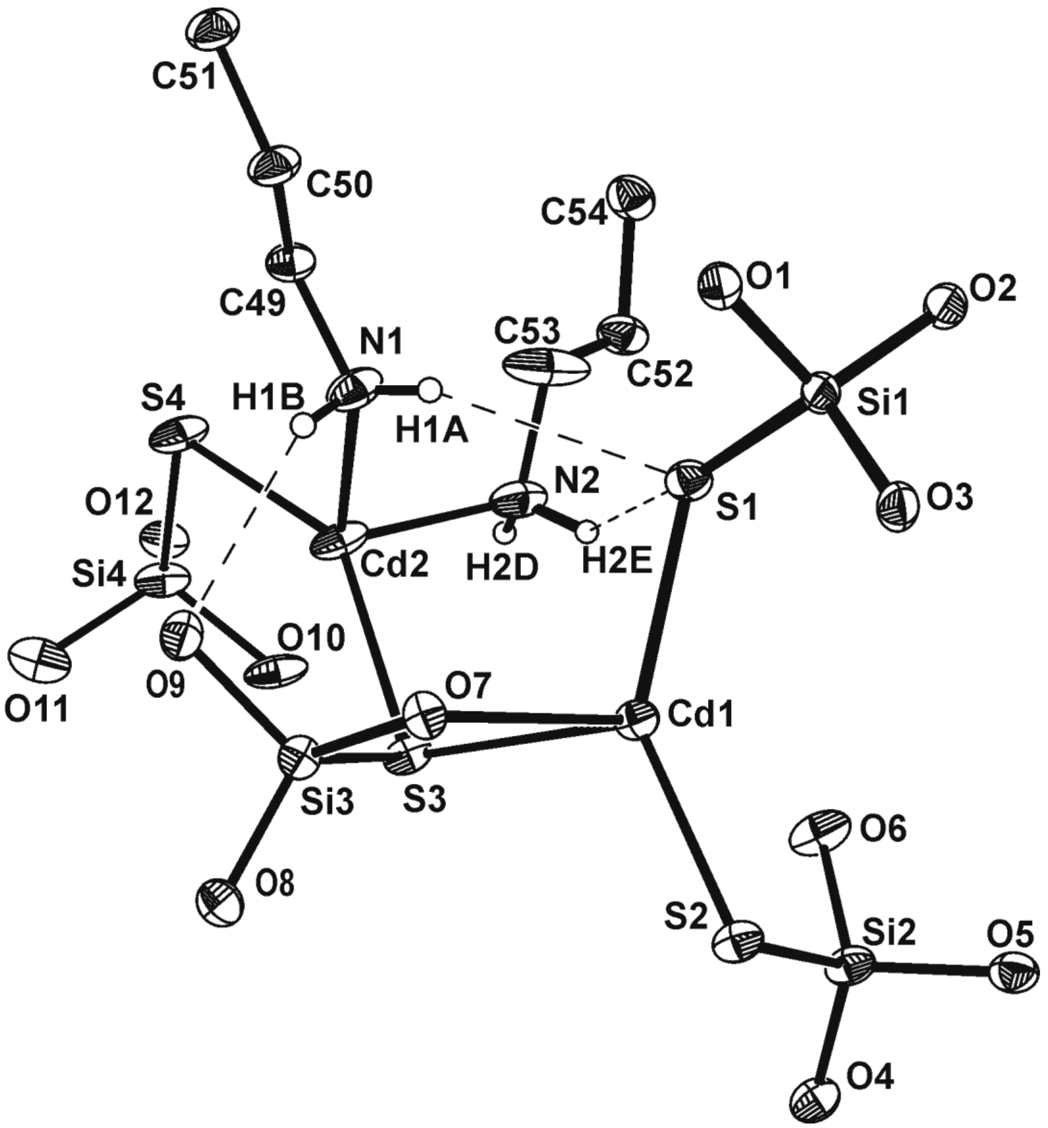

Fig. 4.The core of $[\{SSi(OtBu)_3\}_2Cd\{\mu\text{-}SSi(OtBu)_3\}Cd\{SSi(OtBu)_3\}(\mu\text{-}C_6H_{16}N_2)]_n$ **(3)** with atom labeling scheme and the illustration of two hydrogen bond motifs: $S^1_2(6)$ formed by N1–H1A···S1 and N2–H2E···S1 and $S^2_2(8)$ formed by N1–H1A···S1 and N1–H1B···O9 hydrogen bonds. H atoms of C–H bonds omitted for clarity. Thermal ellipsoids are drawn at 30% probability.

Unlike to **(1)** and **(2)**, compound **(4)** does not contain any molecules of solvent in crystal structure. Nevertheless the net of intra- and intermolecular hydrogen bonds is also present here. One from two hydrogen atoms of each NH_2 forms intramolecular N–H···O hydrogen bond with O atom of *t*BuO group, whereas the second H atom is engaged in intermolecular N–H···S of silanethiolate group from the neighboring polymeric chain (Fig. 5).

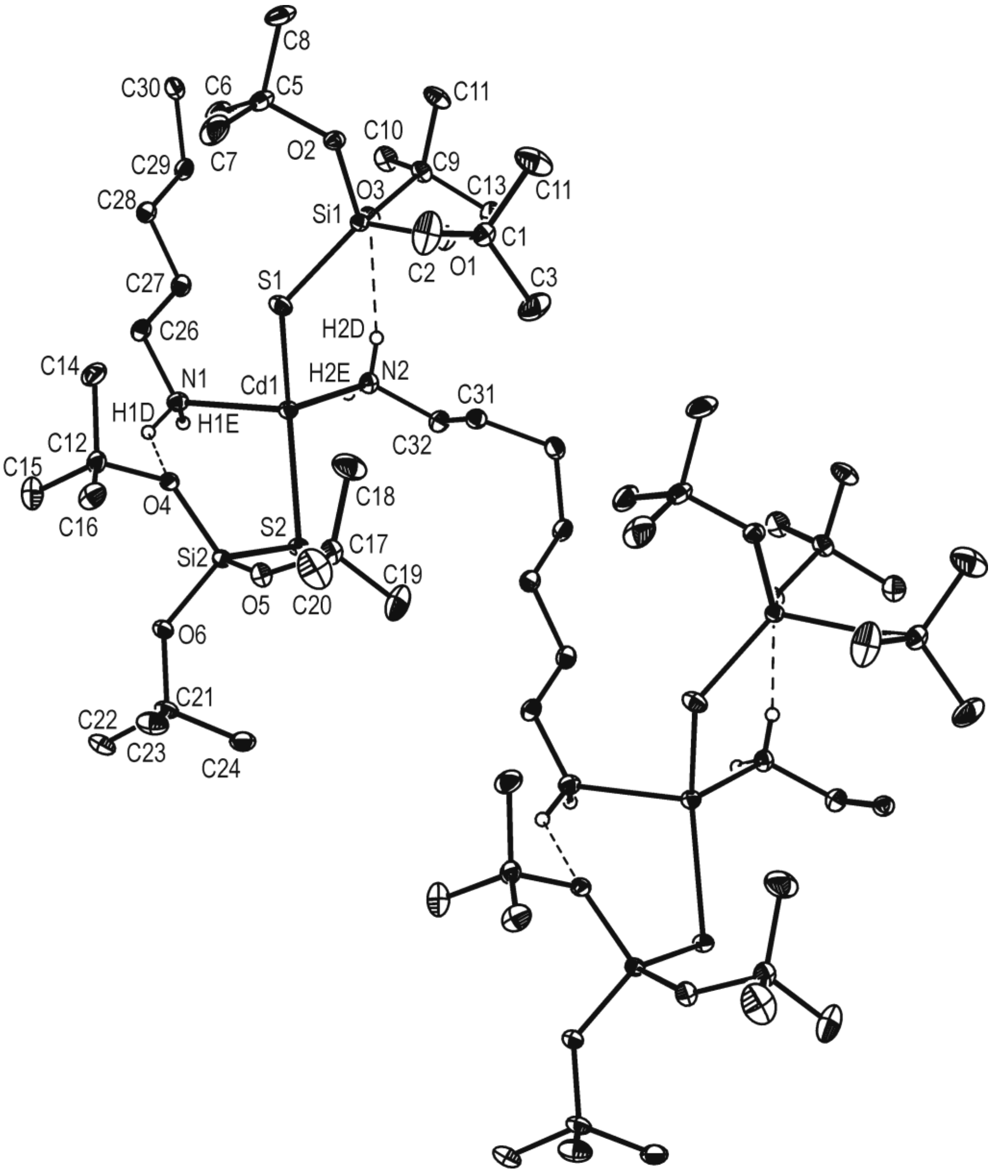

Fig. 5. Molecular structure of $[Cd\{SSi(OtBu)_3\}_2(\mu\text{-}C_7H_{18}N_2)]_n$ **(4)** with atom labeling scheme and hydrogen bond interactions (shown as dashed lines). H atoms of *t*BuO groups are omitted for clarity. Thermal ellipsoids are drawn at 30% probability.

The chains of diamine in **(4)** are bent in the form of a sinusoidal wave and are at a distance of about 4 Ǻ in the adjacent polymeric threads (Fig. S4 Supplementary Materials). Such arrangement of ligands around metallic centers additionally allows for the formation of one weak Cd(1)····O(4) (3.086 Ǻ) interaction between oxygen atom from siloxyl residues and Cd(1). It may have the influence on the angles values around metallic center which are slightly wider in **(4)** (102.05(10)-130.22(3)°) than in **(2)** (98.41(16)-124.01(5)°) (Table 2). The Cd···Cd contacts are only slightly longer in **(4)** (10.211 Ǻ) than in **(2)** even though the N-to-N distances in two bridging ligands differ significantly (mean 7.477Å in 1,5-diaminapentane *vs*. mean 8.703 Å in 1,7-diaminaheptane). Apart from structural disparities the average Ni–N, Ni–S, S–Si and Si–O bond distances in **(1)**, **(2)** and **(4)** complexes are comparable (Table 2).

A different coordination mode has been found in the structure of $[Cd_2\{SSi(O\mathit{t}Bu)_3\}_4(\mu\text{-}C_6H_{16}N_2)]_n$ **(3)**. This complex crystallizes in monoclinic space group C2/c with four molecules in a unit cell (Fig. S3 Supplementary Materials). While it is true that the coordination sphere on metal center in the polymeric chain is the same as in the previous complexes (CdN_2S_2), compound **(3)** contains additional Cd(1) metallic center what distinguishes it from the previous complexes. Cd(1) in **(3)** is coordinated by two silanethiolate residues as S-terminal ligands and one in a O,S-chelating mode (Fig. 4). Sulfur atom from this residue coordinates at the same time to Cd(2) as terminal ligand. The resultant tetrahedral ring Cd(1)O(7)S(3)Si(3) is practically planar, which is typical of cadmium complexes containing tri-*tert*-butoxysilanethiolate residue acting as O,S-chelating ligand [49-51]. In the result the coordination sphere on Cd(1) ion is $CdOS_3$. The only structural consequence of the presence of those additional interactions is the significant elongation of Cd(1)–S(3) bond from chelating tri-*tert*-butoxysilanethiolate residue (2.6555(7) Å) which bridges two Cd(1) and Cd(2) metallic centers through sulfur (Table 3). Additionally the specific spatial arrangement of the ligands around the Cd(1) and Cd(2) facilitate the formation of two additional Cd(1)····O(6) and Cd(2) ····O(10) interactions (2.970 Å and 2.893 Å, respectively). They are shorter then the analogous interactions in complex **(4)**, but also longer then the average Cd–O bond distance (2.36 Å) and even longer than those found in other cadmium silanethiolates (2.5137(13)-2.6165(19) Å) [41, 42, 49-51]. Therefore we considered them not as covalent bonds but as a Cd···O interactions..

The polymeric chain of **(3)** adopts the topology of helix with the twist of N–Cd–N angle. The diamine carbon chain is arranged in a quite regular way (Fig. S3 Supplementary Materials). The possible cause of this order is the presence of three intramolecular hydrogen bonds. Two of them N1–H1A···S1 and N2–H2E···S1 link together to form $S_2^1(6)$ motif, whereas the third hydrogen bond N1–H1B···O9 forms $S_2^2(8)$ motif with N1–H1A···S1 (Fig. 4) [50].

The N-to-N distance in 1,6-diaminehexane is practically the same like in 1,7-diaminaheptane (mean 8.606Å in 1,6-diaminahexane *vs*. mean 8.721 Å in 1,7-diaminaheptane), but the Cd···Cd contacts in resultant polymers differ significantly (12.316 Å in **(3)** and 10.211 Å in **(4)**). Nevertheless it does not affect the Cd–S, Cd–N and Si–S distances and angles in **(3)** which are situated in the average range of values and comparable with those found in heteroleptic monometallic cadmium tri-*tert*-butoxysilanethiolates (Table 3).

The last neutral polymer with the formula of $[Cd_2\{SSi(OtBu)_3\}_4(\mu\text{-}C_8H_{20}N_2)]_n$ **(5)** has been obtained with the use of 1,8-diamineoctane. The reaction of diamine with cadmium binuclear substrate $[Cd\{SSi(OtBu)_3\}_2]_2$ does not change it's structural arrangement only the amine molecule completes the coordination sphere on each metal atom resulting with $CdNS_3$ kernel (Fig. 7). The closer look into the structure of **(5)** shows that O(1) and O(6) atoms from two silanethiolate ligands are slightly directed to the Cd(1) and Cd(2) atoms and are distant at 3.203 Å and 3.408 Å from Cd(1) and Cd(2) respectively. Those distances are significant and cannot be assigned as a covalent bonds but only as a weak interactions.

Complex **(5)** crystallizes in monoclinic space group $P2_1$ with two molecules in a unit cell (Fig. S5 Supplementary Materials). The Cd···Cd and N-to-N distances between next monomers are the longest within obtained **(1)**-**(5)** complexes (15.484 Å and 11.303 Å respectively) according to expectations. The Cd–S bond distances in the Cd_2S_2 ring of complex **(5)** are comparable with those present in substrate $[Cd\{SSi(OtBu)_3\}_2]_2$ and only the Cd(1)···Cd(2) distance in this ring elongated a bit in **(5)**. The coordination of diamine on metallic centers in **(5)** influences also on S(2)–Cd(1)–S(4) and S(2)–Cd(2)–S(4) angles causing their insignificant widening, whereas Cd(1)–S(2)–Cd(2) as well as Cd(1)–S(4)–Cd(2) angles narrowed considerably (84.90(3)° and 84.96(3)°) when compare with the substrate (86.9(1)°) [45]. Diamine molecules are engaged in two intramolecular N–H···O hydrogen bonds with siloxyl residues (Table 4) and are slightly arcuate. Molecules of **(5)** pack into sheets with the separation distance of 14 Å between diamine chains of two neighboring polymeric threads (Fig. 5S Supplementary Materials). Resultant spaces between polymeric fibers are bordered on each site by *t*BuO groups of silanethiolate residues. Figures 6 and 8 are given for better comparison of **(1)**-**(5)** chains topology.

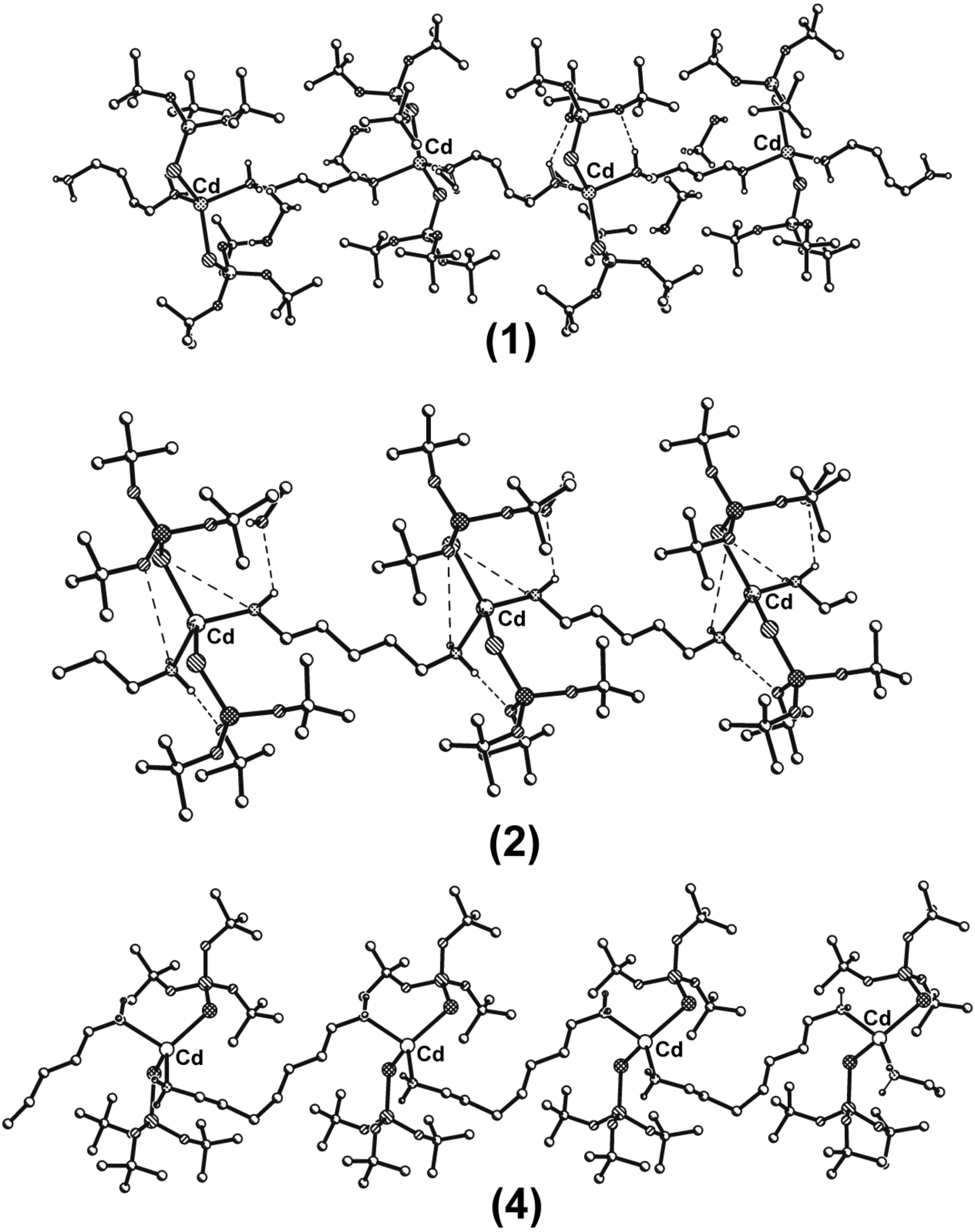

Fig. 6. The comparison of chains topology of complexes **(1)**, **(2)** and **(4)**.

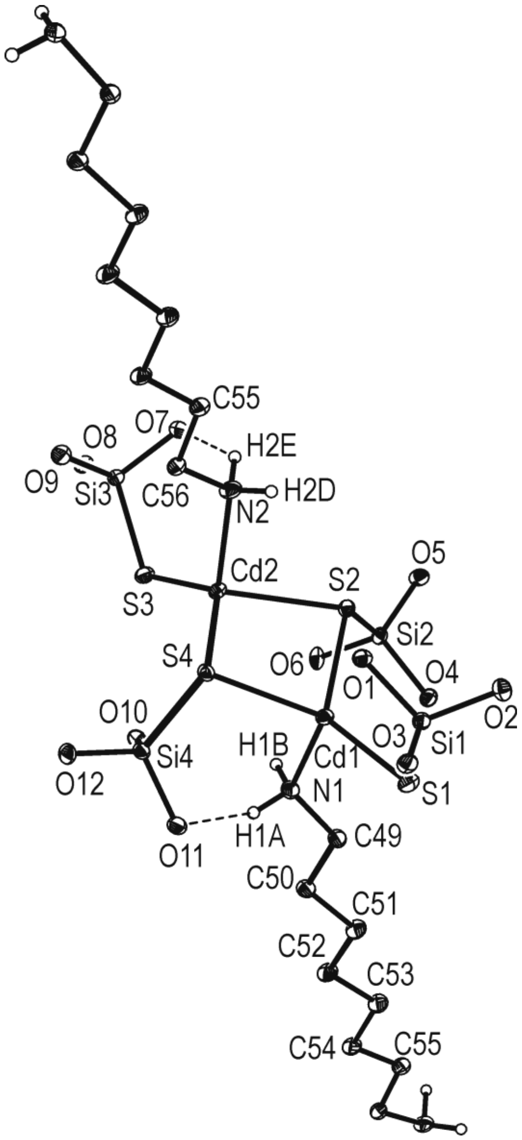

Fig. 7. Molecular structure of $[Cd\{\mu\text{- }SSi(OtBu)_3\}\{SSi(OtBu)_3\}(\mu\text{-}C_8H_{20}N_2)]_n$ **(5)** with atom labeling scheme. All *t*Bu groups and hydrogen atoms of C–H bonds are omitted for clarity. Thermal ellipsoids are drawn at 30% probability.

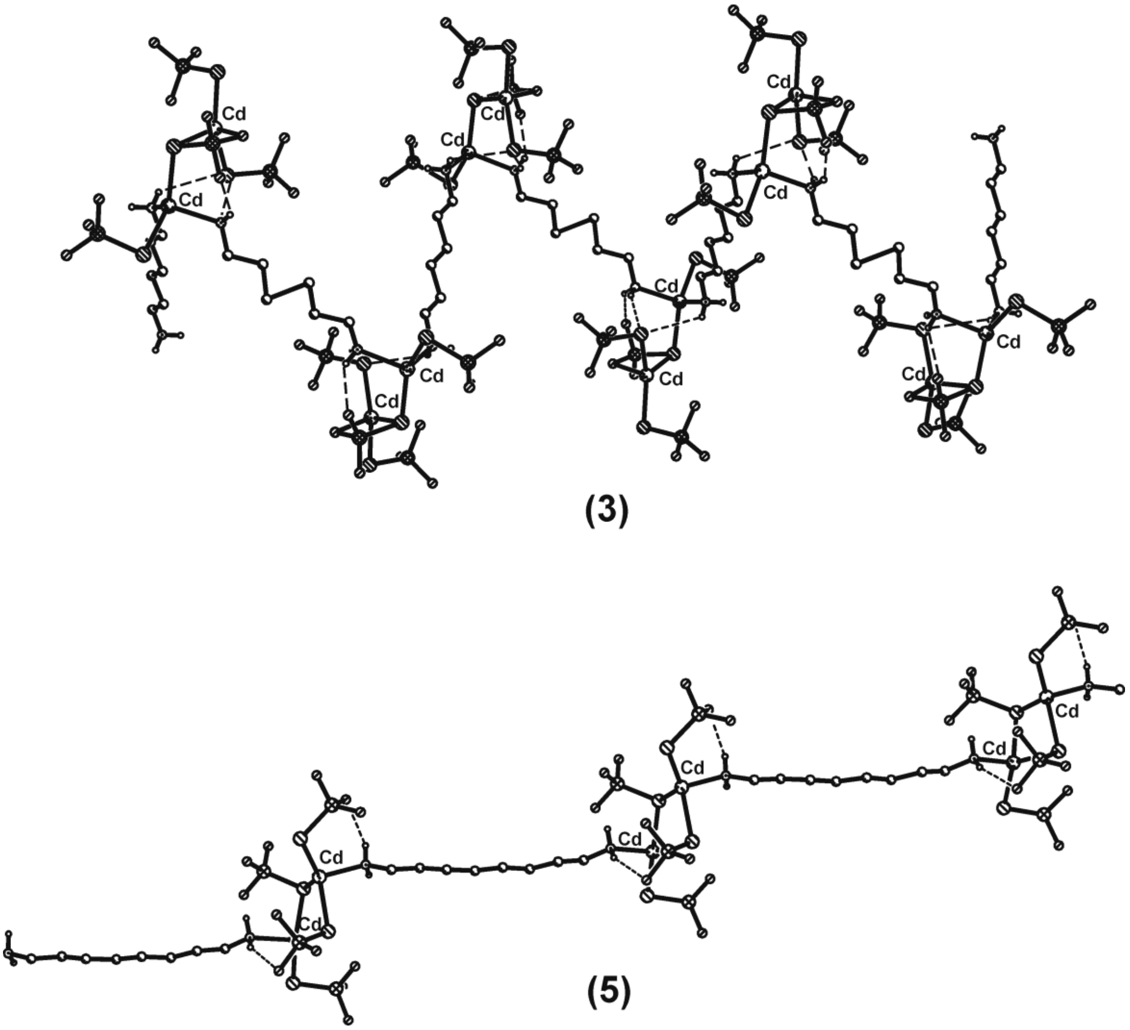

(3)

(5)

Fig. 8. The comparison of chains topology of complexes **(3)** and **(5)**.

3.2. Spectral Characterization.

Vibrational spectra were recorded for complexes **(1)-(5)** in the solid state in the range of 4000-700 cm^{-1} and are consistent with their crystal structures. All five compounds show the characteristic band of NH_2 group vibration at about 3300 and 3400 cm^{-1} corresponding to $\nu_s(NH_2)$ and $\nu_{as}(NH_2)$, respectively (Fig. 9).

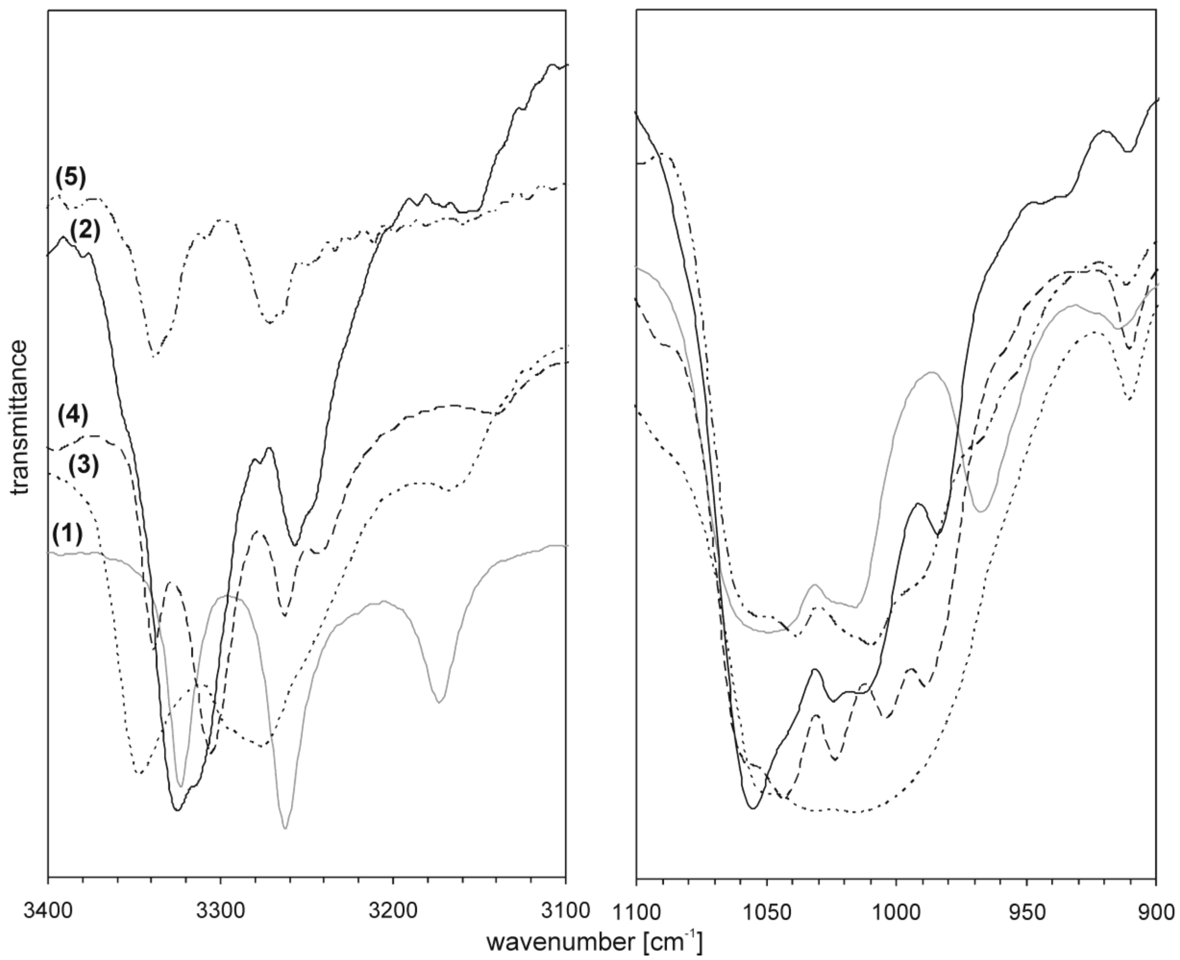

Fig. 9. Solid state FT-IR spectra of **(1)-(5)** in the 3400-3100 cm^{-1} and 1100-900 cm^{-1} range.

The OH stretching vibrations from the solvent should also be present at the same region, but it is difficult to assign those vibrations with particular value. Generally free methanol molecules should show one band at 3682 cm^{-1} but this frequency is red shifted at around 3300 cm^{-1} when the same hydroxyl group is engaged in interactions via hydrogen bonding. An increasing strength of those hydrogen bonding, i.e., liquid and solid state of methanol, led to a further red shift of the OH stretching vibration to 3200 cm^{-1} [53].

The FTIR frequencies of **(1)-(5)** complexes are red shifted due to different structures of analyzed complexes and the presence of intramolecular N–H···S and N–H···O as well as intermolecular N–H···O, N–H···S and O–H···O hydrogen bonds in crystal structures [53, 54]. More similarities can be found in the range of 1100-900 cm^{-1} where complexes show superimposed bands assigned to Si–O–C bonding from silanethiolate residue (Fig. 9). Only spectrum of complex **(3)** show a broad band which is typical for silanethiolates that contain the additional interactions of oxygen from the Si–O–^{t}Bu residue to the metal center.

3.3. Thermal analysis (TG and DTG)

Thermal analysis was followed for **(1)**, **(3)** and **(4)** complexes and TG and DTG curves are shown in Fig.10, 11 and Figs. S6, S8 Supplementary Materials. Thermal diagrams reveal mass loss in the temperature range of 25-400 °C and show that one stage decomposition takes place in case of **(3)** and **(4)** complexes, whereas decomposition of complex **(1)** goes in two-step process which is connected to the presence of solvent molecule in the structure of this complex in contrast to **(3)** and **(4)**. The first noticeable weight loss of **(1)** is at about 160°C what corresponds to the loss of mentioned molecule of CH_3OH (calculated 4.0 %, found 3.6 %) (Fig. 10). Above 180°C gradual weight loss undergoes with final sharp degradation at 294°C with total weight loss corresponding to loss of 89%. A yellow crystalline powder has been obtained as a final solid product of the decomposition of all three complexes and elemental analysis showed the presence of CdS.

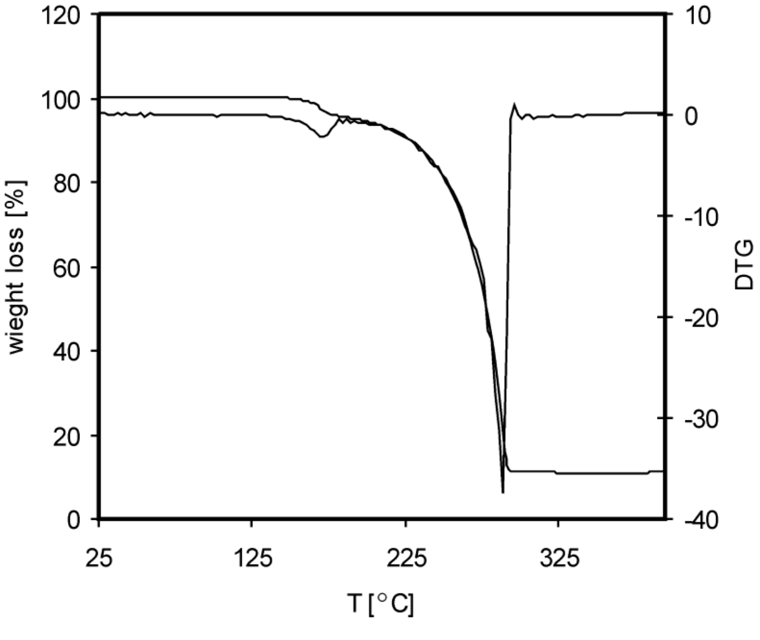

Fig. 10. Thermogravimetric curves of **(1)** for the heating rate of 10 K·min^{-1}.

FTIR spectra of the off-gases of the decomposition process show mostly the same profile for analyzed complexes with the presence of gaseous products that come from the decomposition of tri-*tert*-butoxysilyl substituents (Fig. 11 and Figs S7-S9 Supplementary Materials). They possess both Si–OH ($\nu_{(Si–O)}$=1074 cm^{-1}) and Si–O–*t*Bu ($\nu_{(C–O)}$=1193 cm^{-1}) fragments. Spectra contain also additional bands observed for symmetric and asymmetric scissor-bending vibrations characteristic for *tert*-butyl residues (1394 and 1371 cm^{-1}) as well as for CH_2 groups of aliphatic carbon chains of diamines (1477 cm^{-1}) and skeleton vibration of *t*Bu group (1241 cm^{-1}).

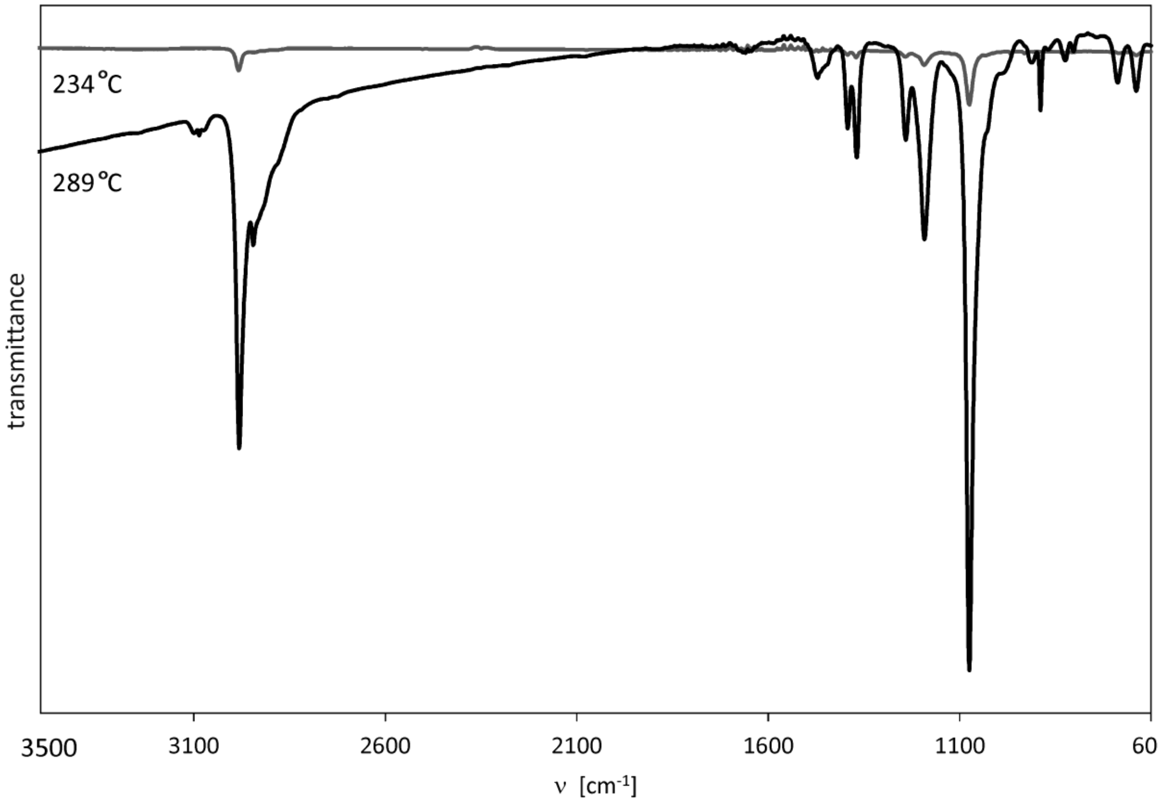

Fig 11. FTIR spectra of the volatiles evolving during TG analysis of **(1)** recorded at 234 and 289 °C.

4. Conclusions:

Five new 1D coordination polymers have been synthesized in the reactions of bimetallic cadmium tri-*tert*-butoxysilanethiolate $[Cd\{SSi(OtBu)_3\}_2]_2$ and various aliphatic, linear diamines. All complexes were characterized by X-ray crystal diffraction, elemental analysis and FTIR measurements. In order to determine the thermal stability, TG and DTG were followed for complexes **(1)**, **(3)** and **(4)**. Also gaseous products from decomposition of those complexes were identified by means of IR spectroscopy. Polymeric chains of presented compounds adopt different chain topologies and contain different amount of metal ions. The

Cd(II) center in polymer threads of **(1)**, **(2)** and **(4)** complexes resides in a CdN_2S_2 environment, whereas complexes **(3)** and **(5)** contain an additional metal center tetrahedrally coordinated with CdN_2S_2 and $CdOS_3$ kernels in **(3)** and $CdNS_3$ in **(5)**. Presented complexes are stable in atmospheric conditions. Despite the structure diversity of described complexes there is still much experimental work required in order to establish strategies disclosing structure correlations and used ligands in the synthesis of coordination polymers that contain silanethiolate ligands.

Appendix A. Supplementary data

CCDC 826670 (compound 1); CCDC 874406 (compound 2); CCDC 874407 (compound 3); CCDC 874408 (compound 4); CCDC 874409 (compound 5) contain the supplementary crystallographic data. These data can be obtained free of charge via http://www.ccdc.cam.ac.uk/conts/retrieving.html, or from the Cambridge Crystallographic Data Centre, 12 Union Road, Cambridge CB2 1EZ, UK; fax: (+44) 1223-336-033; or e-mail: deposit@ccdc.cam.ac.uk. Supplementary data file contains packing diagrams of compounds **(2)-(5)**.

Appendix B. Supplementary data

Supplementary data associated with this article can be found, in the online version, at doi:

Acknowledgement

Financial support from the Polish Ministry of Science and Higher Education Grant No. N N204 155940 is gratefully acknowledged.

References:

[1] M. Concepció Capllonch, A. García-Raso, A. Terrón , M. C. Apella, E. Espinosa, E. Molins, J. Inorg. Biochem. 85 (2001) 173-178.

[2] M. Eddaoudi, J. Kim, D. Vodak, A. Sudik, J. Wachter, M. O’Keeffe, O. M. Yaghi, PNAS 99 (2002) 4900-4904.

[3] M. A. Ali, A. H. Mirza, M. Nazimuddin, R. Ahmed, L. R. Gahan, P. V. Bernhardt, Polyhedron 22 (2003) 1471-1479.

[4] Z.-E. Lin, Y.-Q. Sun, J. Zhang, Q.-H. Wei, G.-Y. Yang, J. Mater. Chem. 13 (2003) 447-449.

[5] H. C. Wu, P. Thanasekaran, C. H. Tsai, J. Y. Wu, S. M. Huang, Y. S. Wen, K. L. Lu, Inorg. Chem. 45 (2006) 295-303.

[6] J.-D. Lin, M.-Z. Lin, C.-C. Jia, Z.-Hua Li, S.-W. Du, Inorg. Chem. Comm. 12 (2009) 487-489.

[7] L. Carlucci, G. Ciani, D. Proserpio, Coord. Chem. Rev. 246 (2003) 247-289.

[8] P. Jiang, Z. Guo, Coord. Chem. Rev. 248 (2004) 205-229.

[9] P. Horcajada, C. Serre, M. Vallet-Regi, M. Sebban, F. Taulelle, G. Ferey, Angew. Chem., Int. Ed. 45 (2006) 5974-5978.

[10] S. Kitagawa, R. Matsuda, Coord. Chem. Rev. 251 (2007) 2490-2509.

[11] V. Perades-Garcia, D. Venegas-Yazigi, A. Cabrera, P. Valencia-Galvez, M. Arriagada, D. Ruiz-Leon, N. Pizarro, A. Zanocco, E. Spodine, Polyhedron 28 (2009) 2335-2340.

[12] Y. Ling, L. Zhang, J. Li, S.-S. Fan, M. Du, Cryst. Eng. Comm. 12 (2010) 604-611.

[13] L. Carlucci, G. Ciani, D. M. Proserpio, A. Sironi, J. Am. Chem. Soc. 117 (1995) 4562-4569.

[14] L. Carlucci, G. Ciani, D. M. Proserpio, A. Sironi, Inorg. Chem. 34 (1995) 5698-5700.

[15] O. M. Yaghi, H. Li, J. Am. Chem. Soc. 118 (1996) 295-296.

[16] D. Braga, F. Grepioni, G. R. Desiraju, Chem. Rev. 98 (1998) 1375-1406.

[17] L. Carlucci, G. Ciani, D. M. Proserpio, J. Chem. Soc., Dalton Trans. (1999) 1799-1804.

[18] O. M. Yaghi, H. Li, C. Davis, D. Richardson, T. L. Groy, Acc. Chem. Res. 31 (1998) 474-484.

[19] S. R. Batten, R. Robson, Angew. Chem., Int. Ed. 37 (1998) 1460-1494.

[20] S. A. Barnett, N. R. Champness, Coord. Chem. Rev. 246 (2003) 145-168.

[21] R. Piękoś, W. Wojnowski Z. Anorg. Allg. Chem. 318 (1962) 212-216; A. Herman, B. Becker, W. Wojnowski Z. Anorg. Allg. Chem., 450 (1979) 178-182

[22] B. Becker, W. Wojnowski, K. Peters, E.-M. Peters, H. G. Von Schnering, Polyhedron 9 (1990) 1659-1666.

[23] W. Wojnowski, B. Becker, J. Saßmannshausen, E. M. Peters, K. Peters, H. G. Von Schnering, Z. Anorg. Allg. Chem. 620 (1994) 1417-1421.

[24] J. Chojnacki, B. Becker, A. Konitz, W. Wojnowski, Z. Anorg. Allg. Chem. 626 (2000) 2173-2177.

[25] B. Becker, A. Zalewska, A. Konitz, W. Wojnowski, Z Anorg Allg Chem 627 (2001) 271-279.

[26] M. Kloskowska, A. Konitz, W. Wojnowski, B. Becker, Z. Anorg. Allg. Chem. 632 (2006) 2424-2428.

[27] J. Chojnacki, A. Ciborska, W. Wojnowski, Acta Crystallogr., Sect. C 64 (2008) m240-m242.

[28] A. Ciborska, K. Baranowska, W. Wojnowski, Acta Crystallogr. Struct. Rep. Online E 64 (2008) m46.

[29] E. Jesionka, K. Baranowska, W. Wojnowski, Phosphorus, Sulfur, and Silicon 184 (2009) 1426-1439.

[30] A. Ciborska, K. Baranowska, W. Wojnowski, Acta Crystallogr. Struct. Rep. Online E 65 (2009) m763.

[31] A. Pladzyk, Ł. Ponikiewski, Inorg. Chem. Comm. 20 (2012) 66-69.

[32] A. Dołęga, Coord. Chem. Rev. 254 (2010) 916-937 and references therein.

[33] B. Becker, A. Pladzyk, A. Konitz, W. Wojnowski, Appl. Organometal. Chem. 16 (2002) 517-524.

[34] A. Kropidłowska, J. Chojnacki, B. Becker, J. Inorg. Biochem. 101 (2007) 578-584.

[35] A. Dołęga, K. Baranowska, A. Pladzyk, K. Majcher, Acta Crystallogr., Sect. C 64 (2008) m259-m263.

[36] A. Dołęga, A. Farmas, K. Baranowska, A. Herman, Inorg. Chem. Comm. 12 (2009) 823-827.

[37] A. Dołęga, A. Pladzyk, K. Baranowska, J. Jezierska, Inorg. Chim. Acta 362 (2009) 5085-5096.

[38] A. Pladzyk, J. Olszewska, K. Baranowska, A. M. Dziurzyńska, Trans. Met. Chem. 35 (2010) 821-827.

[39] A. Pladzyk, K. Baranowska, P. Hapter, Trans. Met. Chem. 35 (2010) 373-379.

[40] Ł. Ponikiewski, A. Pladzyk, W. Wojnowski, B. Becker, Polyhedron 30 (2011) 2400-2405.

[41] A. Dołęga, K. Baranowska, A. Pladzyk, Acta Crystallogr. Struct. Rep. Online E 63 (2007) m3072.

[42] A. Pladzyk, A. Dołęga, K. Baranowska, Acta Crystallogr. Struct. Rep. Online E 63 (2007) m1434-m1436.

[43] A. Dołęga, K. Baranowska, Acta Crystallogr. Struct. Rep. Online E 64 (2008) m616-m617.

[44] A. Pladzyk, K. Baranowska, Z. Anorg. Allg. Chem. 635 (2009) 1638-1644.

[45] W. Wojnowski, B. Becker, L. Walz, K. Peters, E. M. Peters, H. G. von Schnering, Polyhedron 11 (1992) 607-612.

[46] M. R. Saber, M. A. M. Abu-Youssef, M. A. S. Goher, B. A. Sabra, A. K. Hafez, A. M.-A. Badr, F. A. Mautner, J. Mol. Struct. 1008 (2012) 17-23.

[47] Oxford Diffraction: CrysAlis CCD and CrysAlis RED, Version 1.171, Oxford Diffraction Ltd, Abingdon, England (2008).

[48] G. M. Sheldrick, Acta Crystallogr., Sect. A 64 (2008) 112.

[49] A. Dołęga, K. Baranowska, J. Gajda, S. Kaźmierski, M. Potrzebowski, Inorg. Chim. Acta 360 (2007) 2973-2982.

[50] A. Dołęga, K. Baranowska, Z. Jarząbek, Acta Crystallogr. Struct. Rep. Online E 64 (2008) m1515.

[51] A. Dołęga, K. Baranowska, D. Gudat, A. Herman, J. Stangret, A. Konitz, M. Śmiechowski, S. Godlewska, Eur. J. Inorg. Chem. (2009) 3644-3660.

[52] M. C. Etter , J. C. MacDonald, Acta Crystallogr., Sect. B 46 (1990) 256-262; J. Bernstein, R. E. Davis, L. Shimoni, N-L Chang, Angew. Chem., Int. Ed. 34 (1995) 1555-1573.

[53] J. Bódis, J. Kornatowski, J. A. Lercher, Acta Univ. Cib. S. F Chemia 9 (2006) 29-38.

[54] I. Nakagawa, R. J. Hooper, J. L. Walter, T. J. Lane, Spectrochim. Acta 21 (1965) 1-14.

One dimensional coordination polymers generated from Cd(II) tri-*tert*-butoxysilanethiolates and flexible aliphatic diamines

Agnieszka Pladzyk*, Katarzyna Baranowska, Katarzyna Dziubińska, Łukasz Ponikiewski

Department of Inorganic Chemistry, Chemical Faculty, Gdańsk University of Technology, Narutowicza Str. 11/12, 80-233 Gdańsk, Poland

Supporting figures

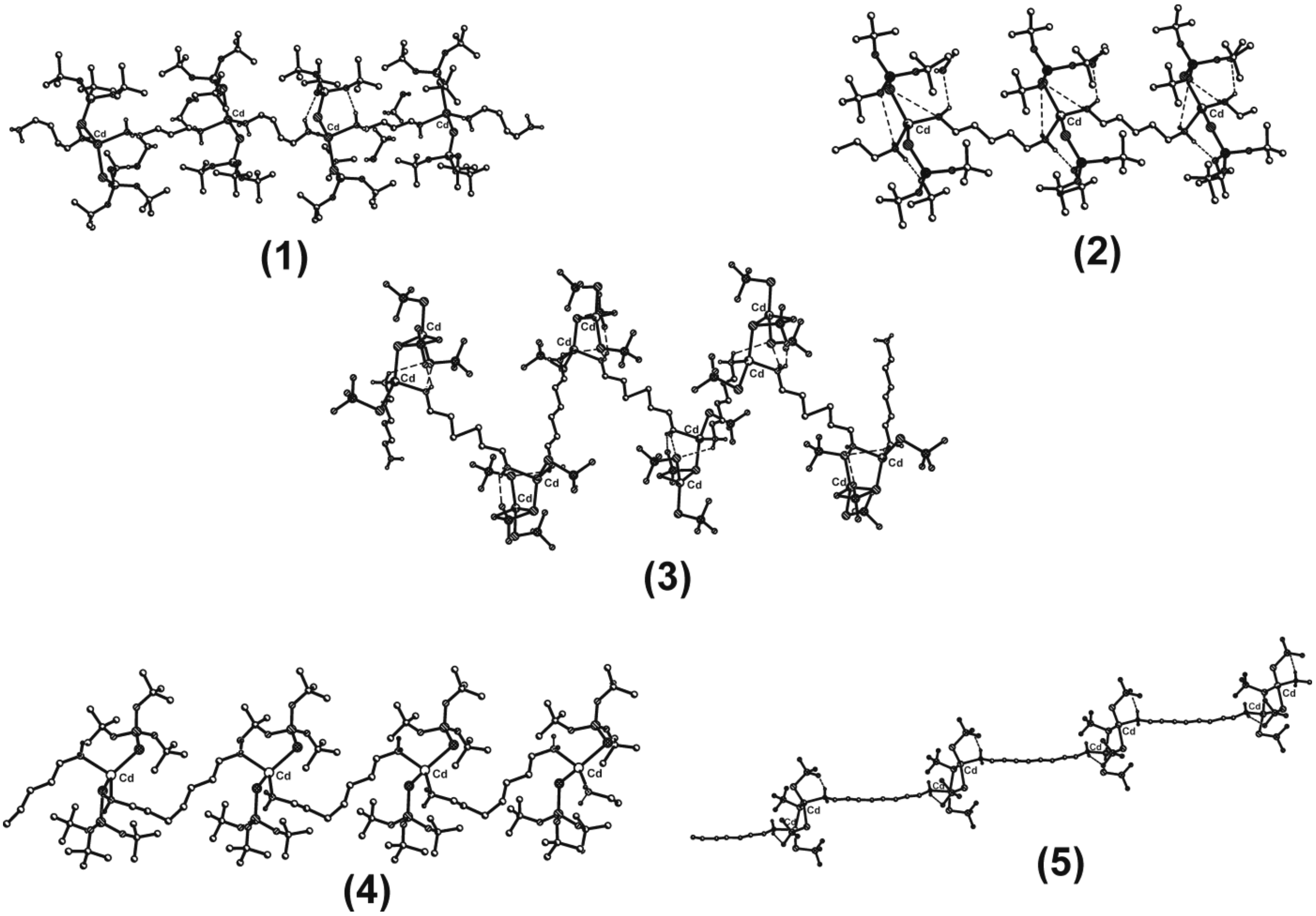

(1)

(2)

(3)

(4)

(5)

Fig. S1. Scheme of **(1)-(5)** complexes.

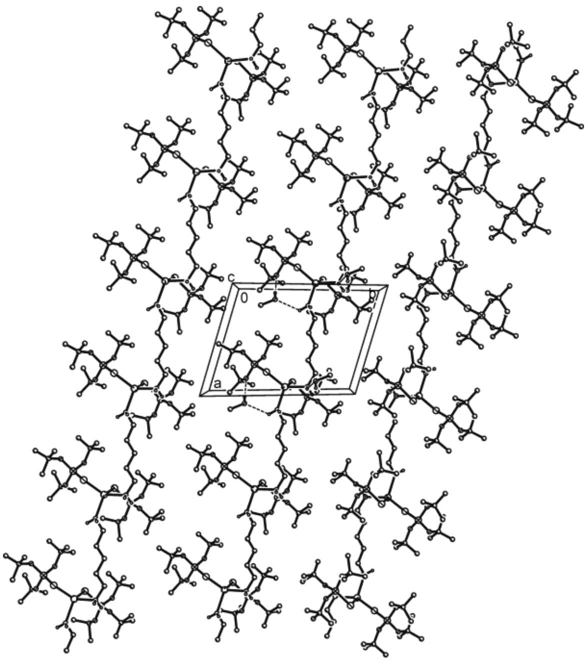

Fig. S2 Crystal packing of **(2)** along c axis. H atoms of *t*BuO groups omitted for clarity.

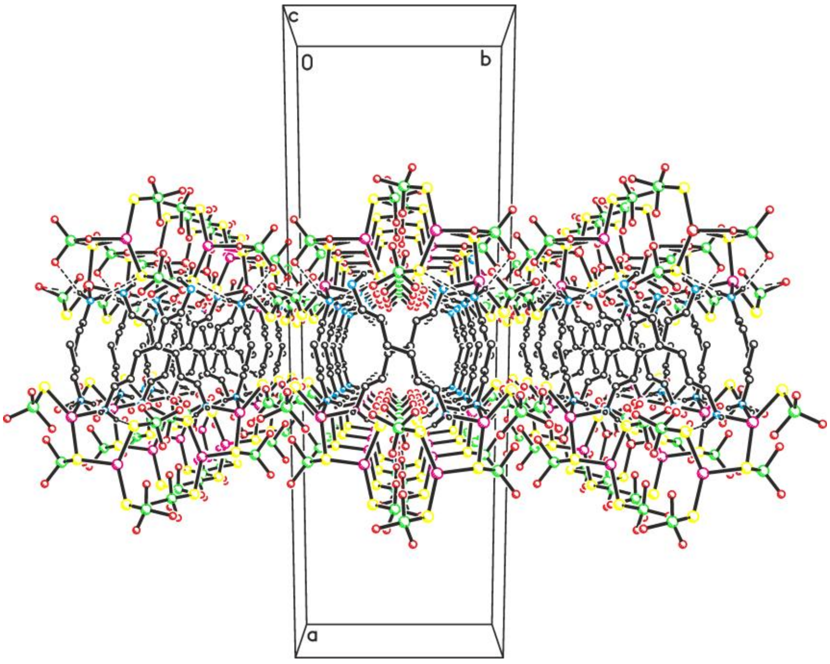

Fig. S3 Crystal packing of **(3)** along *c* axis. *t*BuO groups omitted for clarity (S-yellow, O-red, N-blue, Si-green, Cd-pink, C and H – black).

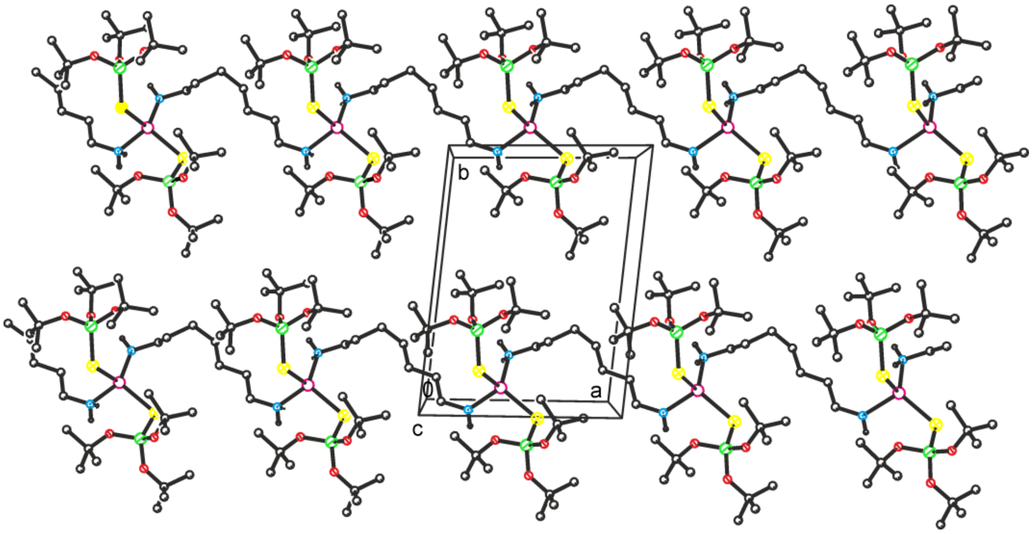

Fig. S4 Crystal packing of **(4)** along *c* axis. H atoms of *t*BuO groups omitted for clarity. (S-yellow, O-red, N-blue, Si-green, Cd-pink, C and H – black)

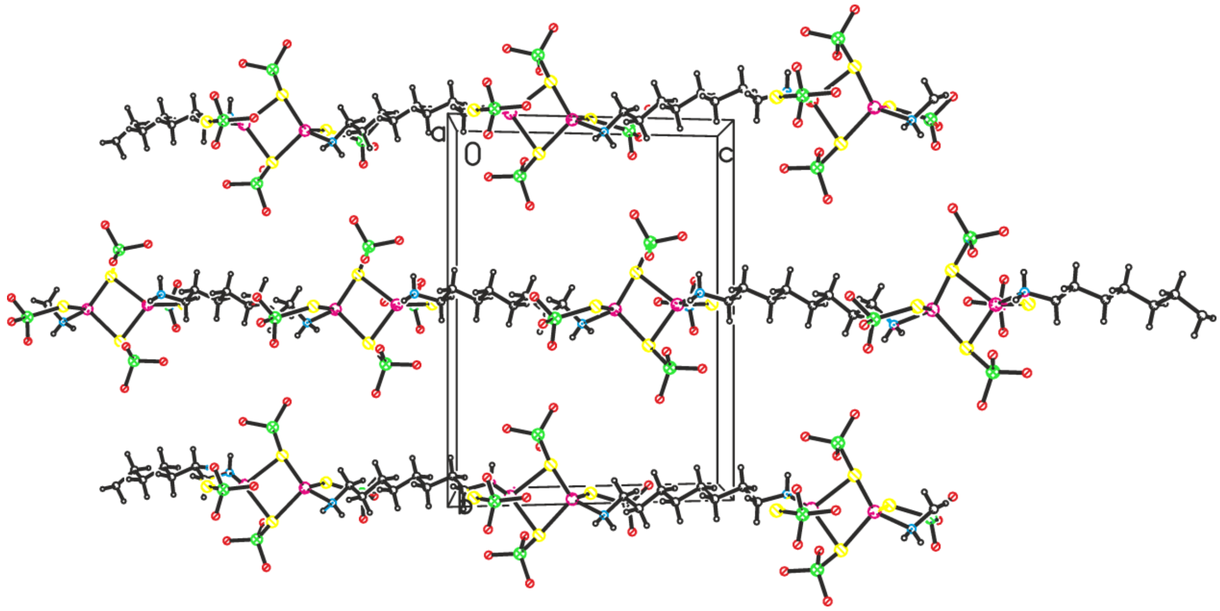

Fig. S5 Crystal packing of **(5)** along *a* axis. *t*BuO groups omitted for clarity. (S-yellow, O-red, N-blue, Si-green, Cd-pink, C and H – black).

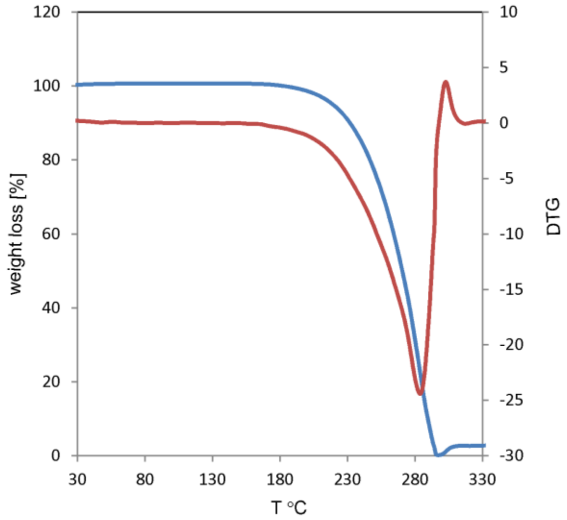

Fig S6 Thermogravimetric curves of **(3)** for the heating rate of 10 K·min^{-1}

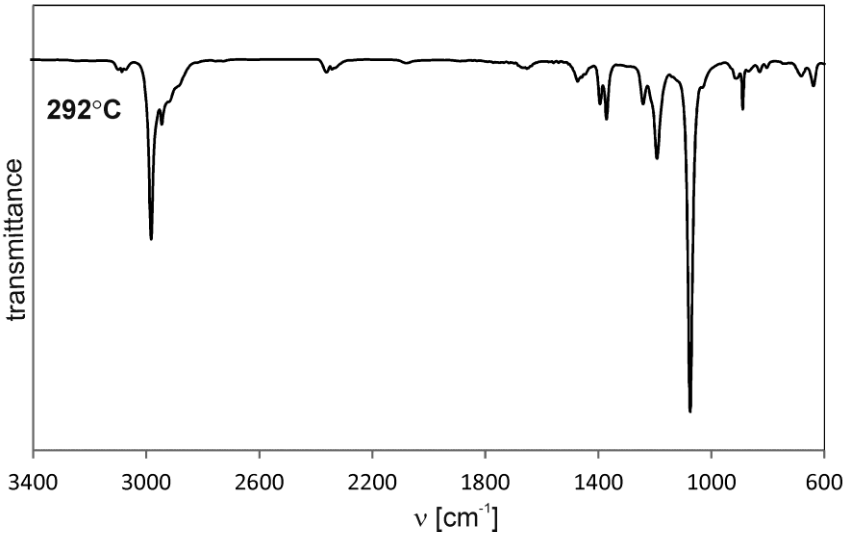

Fig S7 FTIR spectra of the volatiles evolving during TG analysis of **(3)** recorded at 292 °C

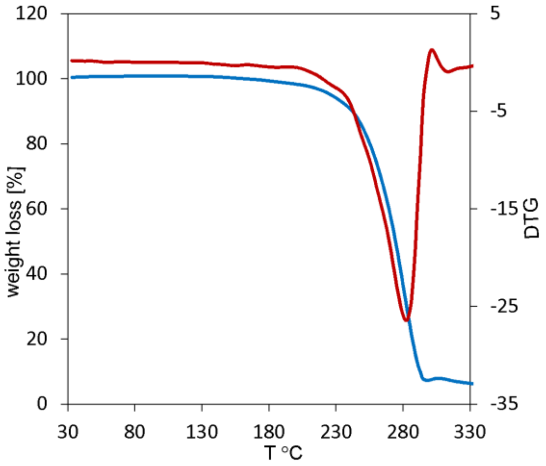

Fig S8 Thermogravimetric curves of **(4)** for the heating rate of 10 K·min^{-1}

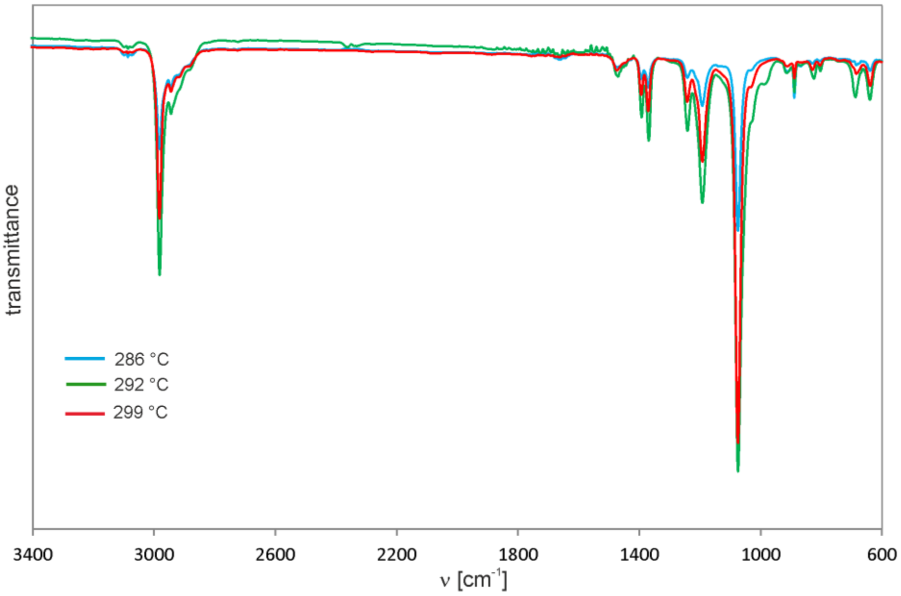

Fig S9 FTIR spectra of the volatiles evolving during TG analysis of **(4)** recorded at 286, 292 and 299 °C.

Table 1 Crystallographic data and structure refinement for **(1)-(5)** complexes

	(1)	**(2)**	**(3)**	**(4)**	**(5)**
Empirical formula	$C_{29}H_{70}CdN_2O_7S_2Si_2$	$C_{30}H_{72}CdN_2O_7S_2Si_2$	$C_{108}H_{248}Cd_4N_4O_{24}S_8Si_8$	$C_{31}H_{72}CdN_2O_6S_2Si_2$	$C_{56}H_{128}Cd_2N_2O_{12}S_4Si_4$
M_r /g mol^{-1}	791.57	805.60	2917.90	801.561	1487.00
Temperature /K	298(2)	120(2)	120(2)	120(2)	120(2)
Wavelength /Å	0.71073 (Mo K_α)	0.71073 (Mo K_α)	0.71073 (Mo K_α)	0.71073 (Mo K_α)	0.71073 (Mo K_α)
Crystal system	monoclinic	triclinic	monoclinic	triclinic	monoclinic
Space group	$P2_1$/c	P–1	$C2/c$	P–1	$P2_1$
a /Å	9.0876(3)	10.0393(3)	48.1097(9)	10.2109(3)	14.0835(3)
b /Å	16.8473(5)	14.6229(6)	14.4214(2)	13.5526(5)	19.4941(4)
c /Å	29.8773(8)	16.8956(5)	25.2096(5)	15.4806(5)	15.3310(4)
α /°	90	113.520(4)	90.0	89.220(3)	90.0
β /°	106.875(3)	96.729(3)	117.382(2)	81.646(3)	109.126(3)
γ /°	90	102.267(3)	90.0	83.857(3)	90.0
V /Å^3	4377.3(2)	2165.15(13)	15531.0(5)	2107.37(12)	3976.71(16)
Z	4	2	4	2	2
D_c (Mg m^{-3})	1.201	1.236	1.248	1.263	1.242
θ range /°	2.34 to 25.50	2.46 to 25.50	2.23 to 25.50	2.26 to 25.50	2.52 to 25.50
Limiting indices	-11<=h<=9 -20<=k<=20 -36<=l<=30	-12<=h<=11 -13<=k<=17 -20<=l<=20	-58<=h<=58 -11<=k<=17 -30<=l<=29	-9<=h<=12 -16<=k<=16 -18<=l<=18	-15<=h<=17 -20<=k<=23 -18<=l<=8
Reflections collected / unique	16311 / 8132 [R(int) = 0.0266]	13419 / 8048 [R(int) = 0.0275]	54085 / 14477 [R(int) = 0.0250]	12998 / 7839 [R(int) = 0.0244]	15643 / 12953 [R(int) = 0.0187]
Completeness to θ_{max} /%	99.9	99.9	99.9	99.9	99.9
μ (mm^{-1})	0.686	0.695	0.765	0.712	0.748
Data / restraints / parameters	8132 / 19 / 412	8048 / 6 / 481	14477 / 8 / 833	7839 / 0 / 431	12953 / 1 / 757
Goodness–of–fit on F^2	1.066	1.092	1.059	1.055	1.051
Final R indices [I>2σ(I)]	R_1 = 0.0742 wR_2 = 0.2042	R_1 = 0.0592 wR_2 = 0.1540	R_1 = 0.0352 wR_2 = 0.0866	R_1 = 0.0386 wR_2 = 0.0950	R_1 = 0.0333 wR_2 = 0.0854
R indices (all data)	R_1 = 0.0823 wR_2 = 0.2115	R_1 = 0.0716 wR_2 = 0.1604	R_1 = 0.0441 wR_2 = 0.0913	R_1 = 0.0469 wR_2 = 0.0984	R_1 = 0.0361 wR_2 = 0.0867
Largest diff. peak and hole /eÅ^{-3}	3.277 and -1.048	2.171 and -0.774	1.189 and -0.832	0.840 and -0.423	1.353 and -0.623

Crystalographic data for the structures **(1)-(5)** have been deposited with the Cambridge Crystallographic Data Centre, CCDC 826670 and 874406-874409. Copies of the data can be obtained free of charge on application to The Director, CCDC, 12 Union Road, Cambridge CB2 1EZ, UK (Fax: int.code +(1223)336–033; e–mail for inquiry: fileserv@ccdc.cam.ac.uk; e–mail for deposition: deposit@ccdc.cam.ac.uk

Table 2. Selected interatomic distances (Å) and angles (°) for **(1)**, **(2)** and **(4)**.

	(1)	**(2)**	**(4)**
Bond lengths			
Cd(1)–N(1)	2.300(7)	2.322(4)	2.326(3)
Cd(1)–N(2)	2.20(2), 2.30(2)	2.302(4)	2.288(3)
Cd(1)–S(1)	2.4790(14)	2.5045(14)	2.4430(8)
Cd(1)–S(2)	2.4525(15)	2.4445(14)	2.4981(8)
Si(1)–S(1)	2.079(2)	2.076(2)	2.0736(11)
Si(2)–S(2)	2.088(2)	2.076(2)	2.0973(11)
Si(1)–O(1)	1.642(4)	1.626(4)	1.628(2)
Si(1)–O(2)	1.617(4)	1.649(4)	1.636(2)
Si(1)–O(3)	1.636(4)	1.623(4)	1.650(2)
Si(2)–O(4)	1.644(4)	1.644(4)	1.637(2)
Si(2)–O(5)	1.634(4)	1.621(4)	1.621(2)
Si(2)–O(6)	1.624(4)	1.633(4)	1.632(2)
Bond angles			
N(1)–Cd(1)–S(1)	99.84(19)	111.44(12)	103.08(8)
N(1)–Cd(1)–S(2)	103.7(2)	100.58(12)	101.39(7)
N(2)–Cd(1)–S(1)	102.9(11)	99.26(13)	110.18(8)
N(2)–Cd(1)–S(2)	110.1(14)	120.49(12)	106.07(8)
S(2)–Cd(1)–S(1)	124.91(5)	124.01(5)	130.22(3)
N(1)–Cd(1)–N(2)	115.7(8) 114.6(7)	98.41(16)	102.05(10)
Si(1)–S(1)–Cd(1)	98.49(7)	100.57(6)	112.53(4)
Si(2)–S(2)–Cd(1)	106.01(7)	108.95(7)	97.94(4)

Table 3. Selected interatomic distances (Å) and angles (°) for **(3)** and **(5)**.

	(3)	**(5)**
Bond lengths		
Cd(1)–S(1)	2.4472(7)	2.4341(9)
Cd(1)–S(2)	2.4283(6)	2.5737(10)
Cd(1)–S(3)	2.6555(7)	-
Cd(1)–S(4)	-	2.6043(10)
Cd(2)–S(2)	-	2.6124(10)
Cd(2)–S(3)	2.5192(6)	2.4118(8)
Cd(2)–S(4)	2.4668(7)	2.5789(10)
Cd(1)–N(1)	-	2.310(3)
Cd(1)–O(7)	2.5711(16)	-
Cd(2)–N(1)	2.310(2)	-
Cd(2)–N(2)	2.315(3)	2.318(3)
Si(1)–S(1)	2.1024(10)	2.0912(13)
Si(2)–S(2)	2.0949(9)	2.1228(14)
Si(3)–S(3)	2.1165(9)	2.0896(14)
Si(4)–S(4)	2.0825(10)	2.1150(14)
Si(1)–O(1)	1.6355(19)	1.629(3)
Si(1)–O(2)	1.6302(18)	1.634(3)
Si(1)–O(3)	1.6214(19)	1.625(3)
Si(2)–O(4)	1.6298(19)	1.624(3)
Si(2)–O(5)	1.626(2)	1.625(3)
Si(2)–O(6)	1.6386(19)	1.618(3)
Si(3)–O(7)	1.6463(17)	1.641(3)
Si(3)–O(8)	1.6040(19)	1.633(3)
Si(3)–O(9)	1.6311(19)	1.620(3)
Si(4)–O(10)	1.641(2)	1.628(3)
Si(4)–O(11)	1.622(2)	1.634(3)
Si(4)–O(12)	1.6290(18)	1.613(3)
Bond angles		
S(1)–Cd(1)–S(2)	143.22(2)	126.74(4)
S(1)–Cd(1)–S(4)	-	126.34(3)
S(2)–Cd(1)–S(3)	111.24(2)	-
S(1)–Cd(1)–S(3)	104.30(2)	-
S(2)–Cd(1)–S(4)	-	91.85(3)
S(1)–Cd(1)–O(7)	103.97(4)	-
S(2)–Cd(1)–O(7)	97.79(4)	-
S(3)–Cd(1)–O(7)	68.18(4)	-
N(1)–Cd(2)–N(2)	102.73(12)	-
N(1)–Cd(1)–S(1)	-	104.12(9)
N(1)–Cd(1)–S(2)	-	103.39(9)
N(1)–Cd(1)–S(4)	-	100.05(8)
N(1)–Cd(2)–S(3)	102.93(7)	-
N(2)–Cd(2)–S(2)	-	91.45(9)
N(2)–Cd(2)–S(3)	99.02(7)	109.73(9)
N(1)–Cd(2)–S(4)	99.34(7)	-
N(2)–Cd(2)–S(4)	101.87(7)	98.71(9)
S(3)–Cd(2)–S(4)	145.10(3)	129.22(4)
S(2)–Cd(2)–S(3)	-	127.45(3)
S(2)–Cd(2)–S(4)	-	91.55(3)

Cd(1)–S(2)–Cd(2)	-	84.90(3)
Cd(2)–S(4)–Cd(1)	-	84.96(3)
Si(1)–S(1)–Cd(1)	110.50(3)	101.24(4)
Si(2)–S(2)–Cd(1)	97.27(3)	108.23(5)
Si(4)–S(4)–Cd(1)	87.68(3)	101.50(5)
Si(2)–S(2)–Cd(2)	-	114.42(5)
Si(3)–S(3)–Cd(2)	100.74(3)	108.39(5)
Si(4)–S(4)–Cd(2)	94.78(3)	105.62(5)
Cd(1)–S(3)–Cd(2)	108.20(2)	-

Table 4 Parameters of the hydrogen bonds in the complexes **(1)-(5)**.

Compound	Bond	D–H [Å]	H···A [Å]	D···A [Å]	∠DHA [°]
(1)	N1–H1A–O3	0.90	2.28	3.081(8)	148.0
	N2–H2D–O1	0.90	2.41(4)	3.13(5)	137(2)
	N3–H3E–O1^{i}	0.88(2)	2.72(14)	3.31(5)	125(12)
(2)	N1–H1A–O1	0.97(6)	2.43(6)	3.287(7)	147(5)
	N1–H1B–O4	0.96(6)	2.36(6)	3.134(6)	137(5)
	N2–H2D–O7	0.91(3)	2.49(7)	3.080(7)	123(6)
	N2–H2E–S1^{i}	0.90(3)	2.58(4)	3.444(5)	162(6)
(3)	N1–H1B–O9	0.88(4)	2.40(4)	3.136(4)	142(4)
	N1–H1A–S1	0.79(3)	2.71(3)	3.435(3)	153(3)
	N2–H2E–S1	0.87(4)	3.04(4)	3.591(3)	123(3)
(4)	N1–H1E–S2^{i}	0.84(4)	2.75(4)	3.518(3)	153(3)
	N1–H1D–O4	0.92(4)	2.68(4)	3.337(4)	128(3)
	N2–H2E–S2^{i}	0.88(3)	2.74(3)	3.528(3)	149(3)
	N2–H2D–O3	0.85(5)	2.49(5)	3.267(4)	153(4)
(5)	N1–H1B–O9	0.88(4)	2.40(4)	3.136(4)	142(4)
	N1–H1A–O11	0.92	2.23	3.039(4)	146.5
	N2–H2E–O7	0.92	2.50	3.229(4)	136.1

Symmetry codes: i **(1)**. (-x+2,-y+1,-z+2); **(2)**. (-x+2,-y+1,-z+1); **(4)**. (-x+1,-y,-z+1).